ELSEVIER SAUNDERS

POSITRON EMISSION TOMOGRAPHY

PET Clin 2 (2007) 109–123

Current Trends in PET and Combined (PET/CT and PET/MR) Systems Design

Habib Zaidi, PhD, PD[a,*], Abass Alavi, MD[b]

Contemporary molecular imaging technologies are leading to a revolutionary paradigm shift in health care and clinical practice. Within the spectrum of macroscopic medical imaging, sensitivity ranges from the detection of millimolar to submillimolar concentrations of contrast media with CT and MRI, respectively, to picomolar concentrations with PET—a 10^8 to 10^9 difference [1]. The sensitivity of in vivo tracer studies is achieved par excellence with PET, which uses electronic collimation and thereby operates with a wide acceptance angle (particularly when operating in a fully three-dimensional mode) for detecting emitted annihilation photons. Consequently, the sensitivity of PET per disintegration, with comparable axial fields of view, is two orders of magnitude greater than that of single-photon emission computed tomography (SPECT).

The historical development of PET is marked by numerous significant technological accomplishments driven by an unprecedented collaboration between multidisciplinary groups of investigators with backgrounds in the medical sciences, physics, chemistry, mathematics, bioengineering, and computer science [2–4]. PET has become one of the major tools for the in vivo localization of positron-emitting tracers and is performed routinely worldwide using ^{18}F-fluorodeoxyglucose (FDG) to answer important clinical questions including those in cardiology, neurology, psychiatry, and oncology. The latter application contributed largely to the wide acceptance of this imaging modality and its use in clinical diagnosis, staging, and the assessment of tumor response to treatment [5].

The introduction of dual-modality PET/CT systems in the clinical setting in the late 1990s revolutionized the practice of diagnostic imaging [6]. Combined PET/CT systems have been operational for almost a decade since their inception. The complementarity between the intrinsically aligned anatomic (CT) and functional or metabolic (PET) information provided in a "one-stop shop" and the opportunity to use virtually noise-free CT images for attenuation correction of the PET data has contributed to the success of this technology and its wide adoption by the medical imaging community.

On the other hand, combining PET with MRI in a single gantry is technically more challenging

This work was supported by Grant No. SNSF 3100A0-116547 from the Swiss National Foundation.

[a] Department of Radiology and Medical Informatics, Division of Nuclear Medicine, Geneva University Hospital, CH-1211 Geneva, Switzerland

[b] Department of Radiology, Division of Nuclear Medicine, Hospital of the University of Pennsylvania, 3400 Spruce Street, Philadelphia, PA 19104, USA

* Corresponding author.

E-mail address: habib.zaidi@hcuge.ch (H. Zaidi).

1556-8598/07/$ – see front matter

doi:10.1016/j.cpet.2007.10.004

pet.theclinics.com

owing to the strong magnetic fields [7]. Nevertheless, significant progress has been made, resulting in the design of a few preclinical PET scanners and one human prototype dedicated for simultaneous PET/MR brain imaging [8]. This article discusses recent advances in PET instrumentation and the advantages and challenges of multimodality imaging systems. Future opportunities, the challenges facing the adoption of multimodality imaging instrumentation, and its role in biomedical research are also addressed.

Trends in PET instrumentation

The first medical applications of positron radiation focused on the brain owing to the pioneering work of Brownell, Sweet, and colleagues at Massachusetts General Hospital who devised the first apparatus based on coincidence detection to localize brain tumors [9–11]. Likewise, most of the first human PET prototypes were developed specifically for functional brain imaging [12–17]. PET is now used in many other applications and owes its success to clinical oncology in which whole-body scanning has a central role.

In theory, an ideal PET tomograph should have high sensitivity and a high counting rate capability in addition to low dead-time losses and low scatter fraction, and it should provide a uniform and high spatial and energy resolution over the whole sensitive volume, allowing one to reach the highest signal-to-noise ratio (SNR) for the lowest possible injected activity. Significant progress has been achieved in the design of commercial PET instrumentation during the last decade. PET can now reach a spatial resolution of about 4 to 6 mm for whole-body imaging, approximately 2.4 mm for PET cameras dedicated for brain imaging (eg, the high-resolution research tomograph [18]), and submillimeter resolution for female breast [19] and small animal imaging [20].

Novel scintillation crystal-based detection technologies that materialized included the use of new cerium-doped crystals (eg, LSO, GSO, LYSO, $LaBr_3$) as alternatives to conventional bismuth germanate (BGO) crystals [21,22], the use of layered crystals (phoswich detectors) and other methods for depth-of-interaction determination, and a renewed interest in old technologies such as time-of-flight (ToF) PET owing to the development of faster scintillation crystals and electronics that made this approach feasible on commercial clinical systems [23].

The scintillation crystal is one of the most critical components of a PET tomograph [24]. Increased light yield, faster rise and decay times, greater stopping power and improved energy resolution, and the linearity of response with energy, in addition to their low cost, availability, mechanical strength, moisture resistance, and machinability are among the desired characteristics of scintillation crystals [25]. Most of these properties are summarized in Table 1 for selected scintillators currently in use or under development for PET applications [26]. Improvements in these characteristics enable detectors to be divided into smaller elements, increasing resolution and minimizing dead-time losses.

Improvements in spatial resolution can be achieved by designing smaller crystals allowing the acquisition of data with finer sampling. One manufacturer (Siemens Medical Solutions, Knoxville, Tennessee) modified the block detector design by using 13 × 13 crystals, 4 × 4 × 20 mm^3 each instead of an 8 × 8 block of 6.45 × 6.45 × 25 mm^3 crystals, allowing one to reach a transverse spatial resolution close to 4 mm (4.5 mm) at the center

Table 1: **Characteristics of scintillation crystals used or developed specifically for the design of current generation PET imaging systems**

Scintillator	BGO	GSO	LSO	LYSO	LuAP	$LaBr_3$
Formula	$Bi_4Ge_3O_{12}$	Gd_2SiO_5:Ce	Lu_2SiO_5:Ce	$LuYSiO_5$:Ce	$LuAlO_3$:Ce	$LaBr_3$:Ce
Density (g/cc)	7.13	6.71	7.4	7.1	8.34	5.3
Light yield (photons/keV)	9	8	25	32	10	61
Effective Z	75	60	66	64	65	46.9
Principal decay time (ns)	300	60	42	48	18	35
Peak wavelength (nm)	480	440	420	420	365	358
Index of refraction	2.15	1.95	1.82	1.8	1.95	1.88
Photofraction (%)[a]	41.5	25	32.5	34.4	30.6	15
Attenuation length (cm)[a]	1.04	1.42	1.15	1.12	1.05	2.13
Energy resolution (%)[a]	12	7.9	9.1	7.1	11.4	3.3
Hygroscopic	No	No	No	No	No	Yes

[a] @ 511 keV.

of the field-of-view. Fig. 1 shows the two corresponding detector blocks. Fig. 2 illustrates the improvement in image quality and the spatial resolution of clinical brain PET images resulting from the improvement in block detector design and the enhanced performance of PET scanners achieved using a smaller size of the crystals and finer data sampling.

The phoswich approach consists of an assembly of two detectors in a sandwich-like design in which the difference in decay time of the light is used to estimate the depth in the crystal where the interaction occurred [27]. This approach may be implemented with solid-state photodiode readouts, which also allow electronically collimated coincidence counting. This technology improves substantially the off-axis spatial resolution because it is able to roughly halve the uncertainty of the depth-of-interaction determination and hence reduce the parallax error, which is inherent to all radial geometries at the cost of more complex readout electronics (Figs. 3 and 4).

An alternative to the phoswich approach with the goal of reducing parallax error would be to use an axial arrangement of long finely segmented scintillation crystals coupled to highly pixelated photodetectors to allow three-dimensional reconstruction of the interaction point of the annihilation photon. Such a concept could be useful for the design of a high-resolution, Compton-enhanced camera dedicated for brain imaging [28]. This design also increases detection efficiency by reconstructing a significant fraction of events that undergo Compton scattering in the crystals [29]. An important advantage is that the transaxial resolution depends only on the crystal segmentation and not on its chemical composition, whereas the axial resolution is closely related to the scintillator properties.

ToF-PET on the other hand is based on the assessment of a difference of the arrival times of the 511-keV annihilation photons to allow restricting the position of positron emission to a subsection of the coincidence line connecting the two scintillation crystals [30,31]. This technique was suggested and explored with limited success in the 1980s due to the lack of crystals combining the required timing resolution and high stopping power [32]. With the arrival of fast scintillation crystals, ToF is now viable, allowing an improvement in the SNR through incorporation of ToF information into the PET reconstruction process [33–35]. One scanner manufacturer (Philips Medical Systems, Cleveland, Ohio) recently introduced the first commercially available fully three-dimensional PET scanner (The Gemini TF) that achieves ToF capability as well as conventional imaging capabilities [23].

Commercially available, dedicated cylindrical, full-ring PET tomographs (Table 2) are still considered to provide state-of-the-art performance for whole-body scanning [23,36–44], whereas various geometries are suggested for dedicated high-resolution scanning of the brain [18,45–48] and female breast [19,49–60]. The improved performance of dedicated systems when compared with scintillation camera–based systems (eg, PENN-PET [61] or C-PET [62]) is due to their higher overall system efficiency and count rate capability, which provides

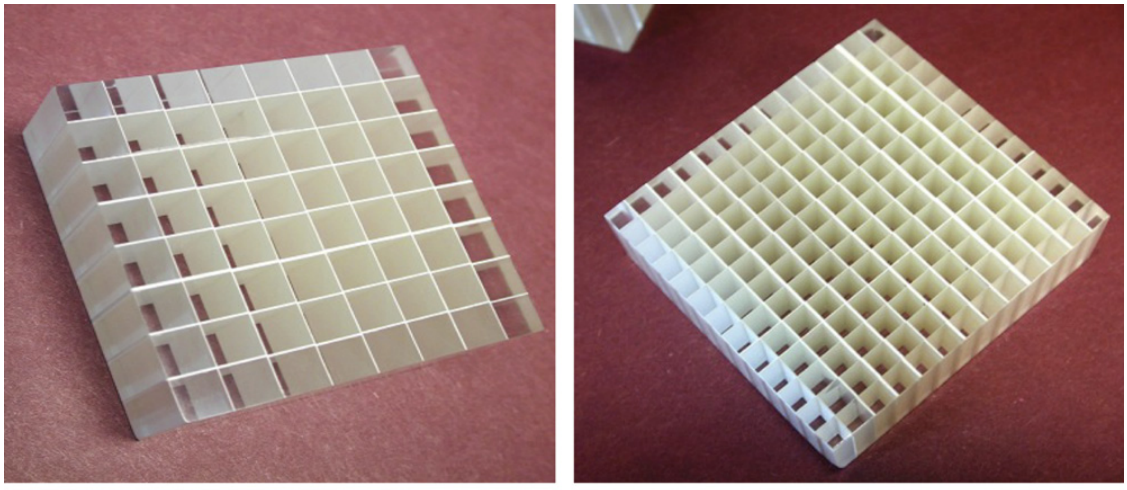

Fig. 1. Photographs of two different geometrical arrangements of PET block detector design realized using an assembly of 8 × 8 crystals of 6.45 × 6.45 × 25 mm^3 each (*left*) and 13 × 13 crystals of 4 × 4 × 20 mm^3, with each crystal allowing one to reach a transverse spatial resolution of 4.5 mm at the center of the field of view (*right*). (*Courtesy of* Siemens Medical Solutions, Knoxville, Tennessee; with permission.)

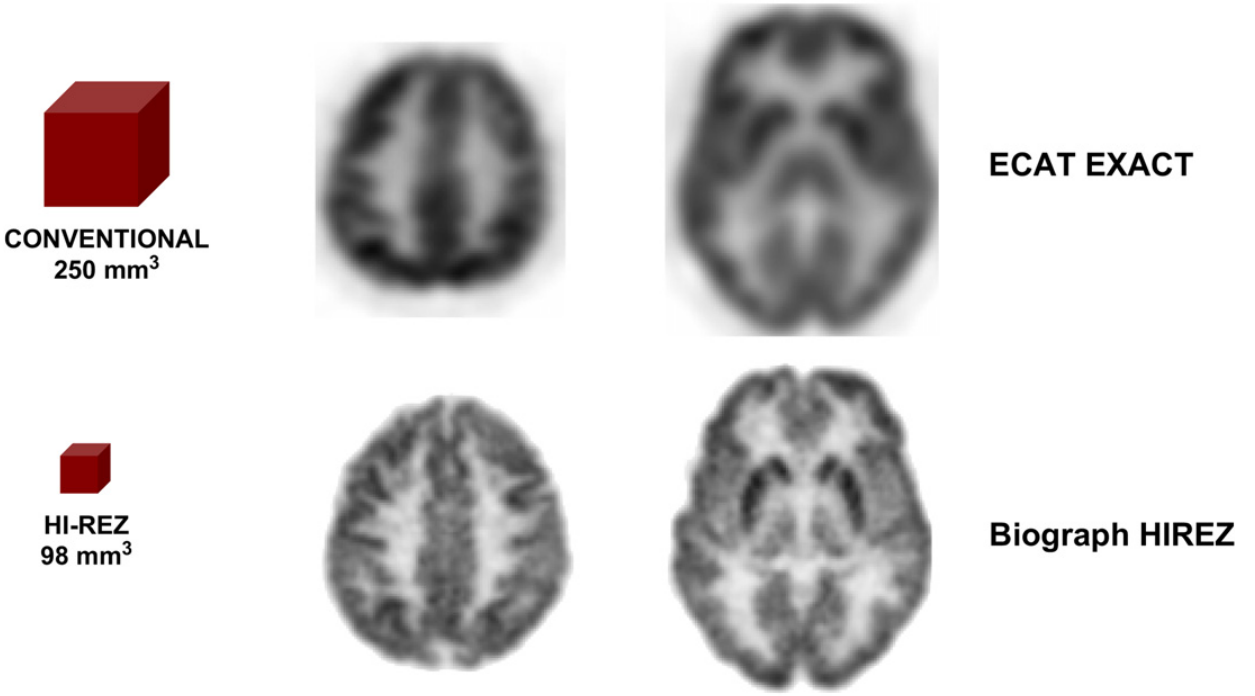

Fig. 2. Representative images of the same patient acquired on the Siemens ECAT EXACT (*top*) and Siemens Biograph Sensation 16 (*bottom*) are shown.

the statistical realization of the physical detector resolution and not a higher intrinsic physical detector resolution [63].

Advances in dual-modality PET/CT imaging

Although dual-modality imaging systems designed specifically for clinical practice are a recent feature, the potential advantages of combining anatomic and functional imaging have been recognized since the early years of medical imaging by radiologic scientists and physicians [64]. Many of the pioneering developers of nuclear medicine instrumentation documented that the capabilities of a radionuclide imaging system could be improved by adding an external source to allow acquisition of transmission data for anatomic correlation of the emission image. Nevertheless, the theoretical concepts were never practically realized in an experimental or a clinical setting until Hasegawa and colleagues [65,66] at the University of California, San Francisco, pioneered in the 1990s the development of dedicated SPECT/CT. Later, Townsend and coworkers (University of Pittsburgh) pioneered in 1998 the development of combined PET/CT imaging systems, which have the capability to record both PET emission and x-ray data for correlated functional/structural imaging [6,67].

Before the commercial introduction of hybrid units (and even after their introduction), much worthwhile research was conducted in the field of software-based multimodality image registration and fusion with the goal of improving the correlation between anatomic (CT and MRI) and physiologic or metabolic (PET) information in clinical and research settings [68,69]. Software-based image registration allows one to fuse images from two or more different modalities after they are acquired separately [70]. The simplest form of image registration uses "rigid-body" translation and rotation to match the two image data sets. These techniques can be applied most successfully to brain studies, where the skull provides a rigid structure that preserves the geometrical relationship of regions within the brain, and have been used since the 1990s for clinical procedures at many facilities [71,72].

The situation becomes more difficult when image registration techniques are applied to other areas of the body, such as the thorax and abdomen, where the body can bend and flex, especially when the PET and CT data are captured in separate procedures using different units located in different facilities, often on different days. Geometrical relationships between different anatomic regions can be affected by the shape of the patient table, the orientation of the body and limbs (up or down) during the imaging procedure, internal organ shift between the two procedures, and the respiratory state of the patient. In these cases, image registration might match the patient anatomy in one region of the body but not in all anatomic regions. Image warping can improve registration over a larger region of the patient's anatomy, but, in most cases, software-based image registration can

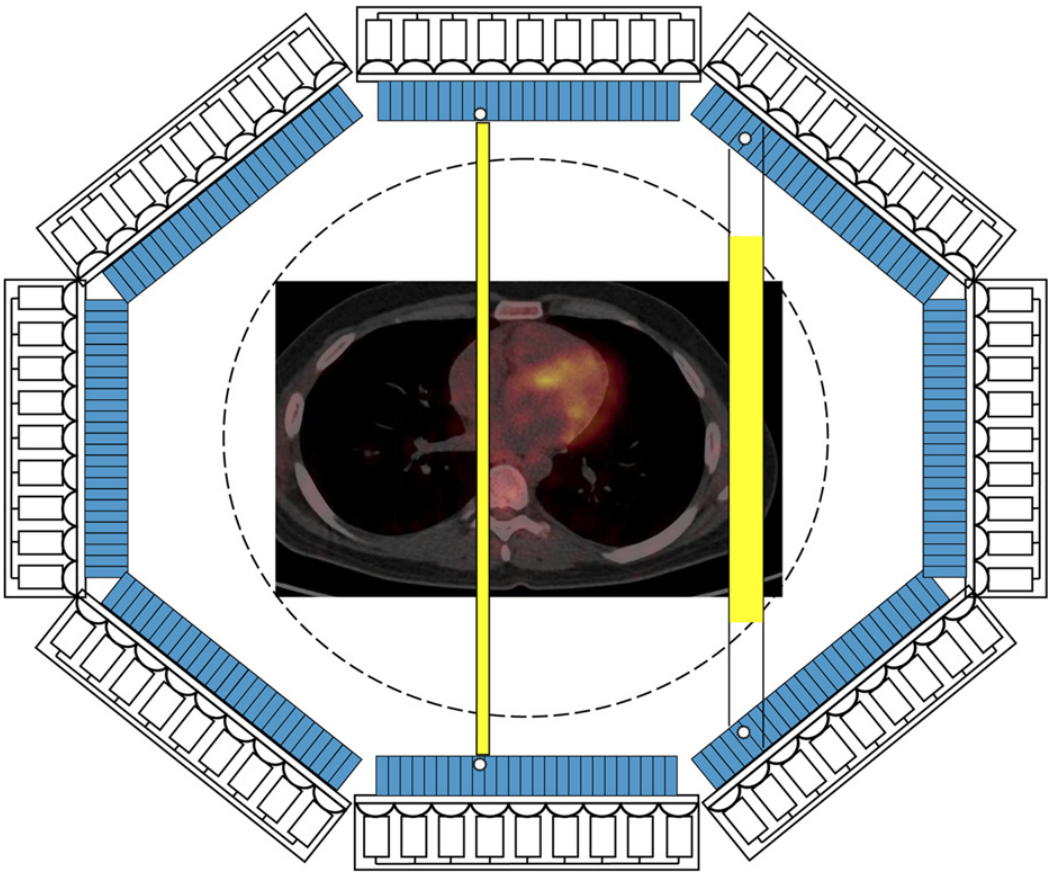

Fig. 3. Illustration of the parallax or depth-of-interaction error associated with annihilations occurring off-center of the transaxial field of view or oblique lines of response for a multi-ring PET scanner. Note the considerable degradation of spatial resolution for off-centered lines of response inherent to all radial geometries.

be challenging and at most institutions is not used routinely for clinical procedures unless the multimodality data can be collected on the same day using carefully matched anatomic positioning and respiration protocols [73,74].

Combined PET/CT might offer a crucial advantage over separate PET and CT imaging systems in correlating functional and anatomic images without moving the patient (except for table translation). Different designs of combined PET/CT tomographs have been developed for diagnostic purposes in clinical oncology and have been commercially available since 2001 [6,75]. This technique produces anatomic and functional images with the patient in the same position and during a single procedure, simplifying the image registration and fusion processes. Fig. 5 shows the essential steps that comprise a typical PET/CT scan, demonstrating the degree of integration available in a contemporary dual-modality imaging system.

In seeking to achieve accurate registration of the anatomic and functional images, combined PET/CT imaging offers several potential advantages over conventional imaging techniques. First, the PET and CT images are supplementary and complementary. PET images allow one to identify areas of disease that are not apparent on the CT images alone [76]. CT images provide an anatomic context that interpreters can use to differentiate normal metabolic uptake from that indicating disease, and to help localize disease sites within the body. Second, the low-noise CT data can be used to generate a patient-specific attenuation map and other a priori anatomic data, which, in turn, can be used to correct the PET data for errors due to photon attenuation [77], scatter radiation [78], and other physical effects or, alternatively, to serve as support during the reconstruction process [79]. In these ways, the CT data can be used to improve the visual quality and the quantitative accuracy of the correlated radiotracer data. Current commercial PET/CT systems consist of multislice spiral CT of up to 64-slice capability allowing cardiac imaging to be performed with a high temporal resolution.

The advent of combined PET/CT units is a prominent example of an advance in molecular imaging technology that offers the opportunity to modernize the practice of clinical oncology by improving lesion localization and facilitating treatment planning for radiation therapy. Nevertheless, several important challenges must be overcome, including dealing with potential artifacts that may arise owing to effects such as respiratory-induced misregistration of the PET and CT data [80–85], truncation

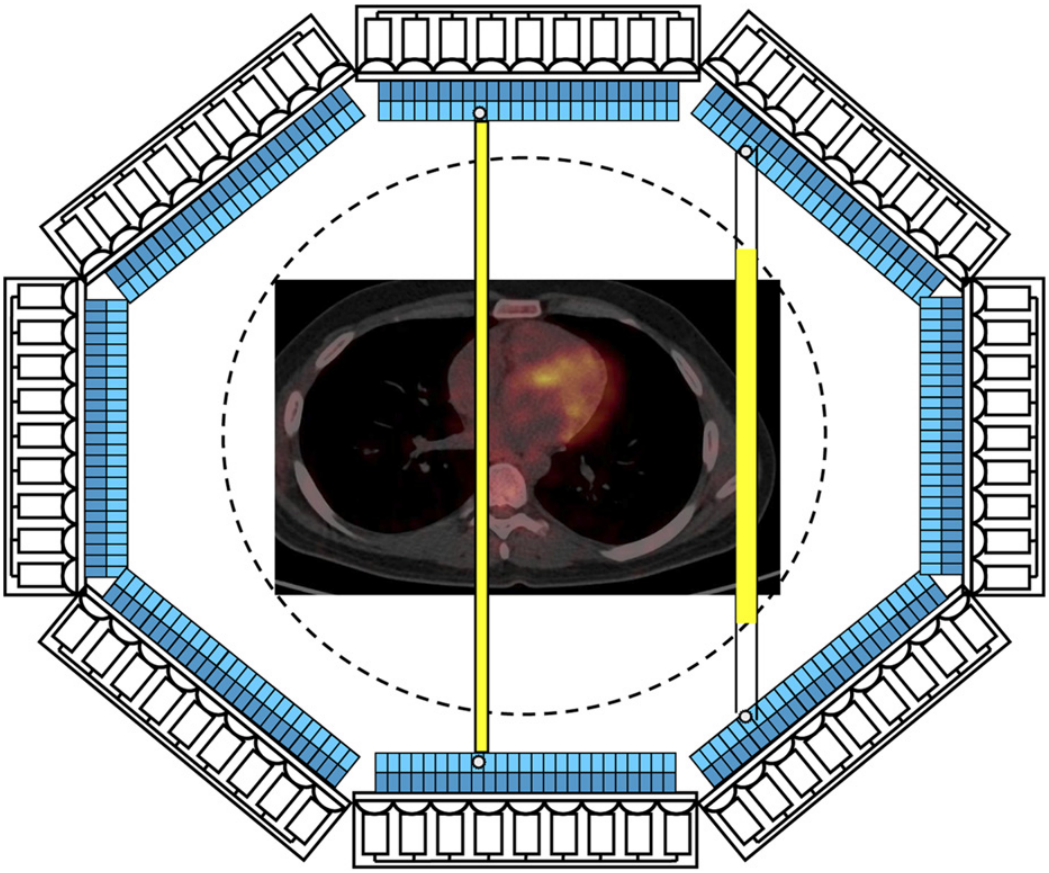

Fig. 4. Illustration of the reduction of parallax or depth-of-interaction error when using the phoswich detector approach with depth-of-interaction measurement capability. The two detectors are assembled in a sandwich-like design in which the difference in decay time of the light is used to estimate the crystal where the interaction occurred, allowing one to roughly halve the uncertainty of the depth-of-interaction. Note the reduction in degradation of spatial resolution for off-centered lines of response.

artifacts owing to discrepancy between fields of view in a dual-modality system [86–89], the presence of oral and intravenous contrast medium [90–99], artifacts due to metallic implants [100–107], beam hardening artifacts caused by the polychromatic nature of CT x-rays [108,109], x-ray scatter in CT images for future generation cone-beam geometries [110–112], and other CT artifacts from any source.

Since its inception, PET/CT has been advertised as a cutting-edge technology to influence clinicians and decision makers to adopt it as the new gold standard modality and to push scanner manufacturers to replace stand-alone PET scanners with combined PET/CT units. The latter is considered a questionable choice by some investigators [113–115]. The marketing strategy of vendors supported by many scientists aiming at disseminating PET/CT technology in the clinic is that the added value of combined units is well-established and represents the ultimate solution for image co-registration. According to these advocates, this solution enables appropriate combination of imaging technologies to yield useful anatomolecular imaging fusion [116]. The bottom line is that, although PET/CT has been accepted commercially, the clinical benefits and the need for this technology remain controversial [117,118] and are still being debated [113,115,119]. Although hybrid PET/CT has many interesting features and offers several advantages when compared with software approaches of image co-registration for patient diagnosis and image-guided radiotherapy, it is often argued that combined PET/CT is not the ultimate solution for image co-registration [73,120,121].

The promise of simultaneous PET/MR imaging

As diagnostic techniques transition from the systems to the molecular level, the role of multimodality imaging will become ever more important. The combination of PET and MRI, enabling truly simultaneous acquisition, will bridge the gap between molecular and systems diagnosis. Both imaging modalities offer richly complementary information about disease; their integration into a combined system offering simultaneous acquisition will capitalize on the strengths of each, providing a hybrid technology that is significantly better than the

Table 2: **Main performance characteristics of commercial PET/CT scanners operating in three-dimensional mode (factory data)**

Parameter	Biograph truepoint	Gemini GXL	Gemini TF	Discovery LS	Discovery ST	Discovery STE/VCT	SceptreP3
CT							
Number of slices	6, 16, 40, 64	6, 16	16, 64	4, 8, 16	4, 8, 16	8, 16, 64 (VCT)	4
Rotation speed (s)	0.33/0.42	0.4	0.4/0.5	0.5	0.5	0.4	0.8
Detector material	UltraFast ceramic	Solid-state GOS	Solid-state GOS	Patented ceramic	Patented ceramic	Patented ceramic	Ceramic
Temporal resolution (ms)	~90	~100	~100/120	~120	~120	~100	~200
Spatial resolution (line pairs/cm)	15.1/24	16/24	24	15.4	15.4	15.4	16
PET							
Scintillation crystal	LSO	GSO	LYSO	BGO	BGO	BGO	LSO
Number of crystals	32,448 (True V)	17,864	28,336	12,096	10,080	13,440	4,224
Detector size (mm)	4 × 4 × 20	4 × 6 × 30	4 × 4 × 22	4 × 8 × 30	6.2 × 6.2 × 30	4.7 × 6.3 × 30	6.45 × 6.45 × 25
Axial field of view (cm)	16.2/21.6 (True V)	18	18	15.2	15.7	15.7	16.2
Sensitivity (cps/kBq)	7.9 (True V)	8	7.2	1.3	2	2	8.7
Peak noise equivalent count rate (kcps)	165 (True V)	70	105	42	63	75	34
Activity concentration @ peak NEC (kBq/cc)	32	11	16	8.5	12	12	—
Scatter fraction (%)	<36	37	30	43	44	35	<36
Transverse resolution @ 1 cm (mm)	4.2	5.3	4.7	4.8	6.2	5.0	6.3
Transverse resolution @ 10 cm (mm)	4.8	6.0	5.1	5.2	6.7	5.6	6.8
Axial resolution @ 1 cm (mm)	4.5	6.0	4.7	6.5	5.6	5.6	5.3
Axial resolution @ 10 cm (mm)	5.5	6.6	5.2	7.5	5.9	5.9	7.0

The characteristics for the two-dimensional mode for some scanners were omitted to facilitate comparison.
Abbreviation: NEC, noise equivalent counts.

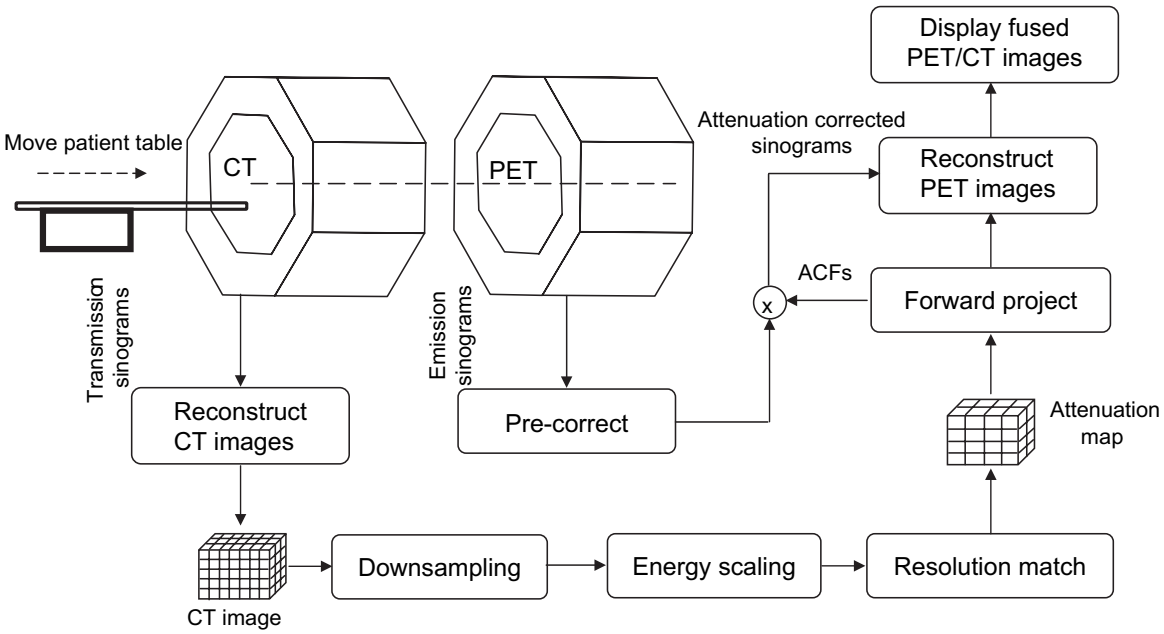

Fig. 5. Principles of operation of a combined PET/CT scanner showing the key hardware components and the main steps involved in data acquisition and processing protocols, including generation of the attenuation map required for CT-based attenuation correction of PET data. ACFs, attenutation correction factors.

sum of its parts. The recent introduction of hybrid PET/MR technology is considered by many experts as a major breakthrough that will potentially lead to a revolutionary paradigm shift in health care and revolutionize clinical practice [122]. Several active research groups in academic and corporate settings are focusing on the development of various configurations of MR-compatible PET inserts to allow simultaneous scanning using the most highly sophisticated molecular imaging technologies available today.

The idea of designing a combined PET/MR system goes back to the mid-1990s, even before the design of the first PET/CT prototype [123–125]. The first attempts to design MR-compatible PET units relied on simple modification of conventional PET detectors for small animal systems to keep the photomultiplier tubes (PMTs) away from the strong magnetic field of MRI [126–131]. In this approach, scintillation crystals were coupled to 3- to 5-m long optical fibers, leading the weak scintillation light outside the fringe magnetic field to position-sensitive PMTs. One major drawback of this design is that the long fibers result in the loss of a significant fraction of the scintillation light, affecting energy and timing resolution, deteriorating crystal identification, and loosing PET signal performance.

Other related approaches based on conventional PMT-based PET detectors rely on more complex magnet designs, including a split magnet [132] or a field-cycled MRI [133]. In the former design, an 8-cm gap in the radial direction of the B_0-field of a 1-T actively shielded superconducting magnet houses the preclinical PET scanner and shorter (1.2 m long) optical fiber bundles [132]. This design allows one to place the PMTs at very low field strength (~30 mT). The major advantage of this design is that only minor modifications of existing conventional PET detectors are required. Nevertheless, the magnet and gradient coil design is more complex and expensive when compared with technologies used on typical MRI scanners. In the latter approach, the PMTs are built into the magnet, but PET scanning is allowed only within small time intervals (~2.5 seconds) when the MR polarizing and readout fields are switched off [133]. The switching cycle for the 1-T polarizing field requires about 1 second to magnetize the object and is shut down very quickly. The hardware implementation of this design still needs to be demonstrated given that the exposure of the PMTs to a variable magnetic field remains challenging. In addition, the use of electromagnets (instead of superconducting magnets) for field-cycled MRI engages significant compromises.

The potential of using novel readout technologies insensitive to magnetic fields, including Avalanche Photodiodes (APDs) and Silicon PMTs (SiPMs), has not yet been fully realized. APD-based technology has been successfully implemented by one small animal PET vendor [134] and in many preclinical PET/MR systems [135–137]. SiPMs, small finely pixilated APDs operated in Geiger mode, have a large potential for further improvement; however, their current performance (high gain and an excellent SNR) is sufficiently good that they can be considered strong candidates in

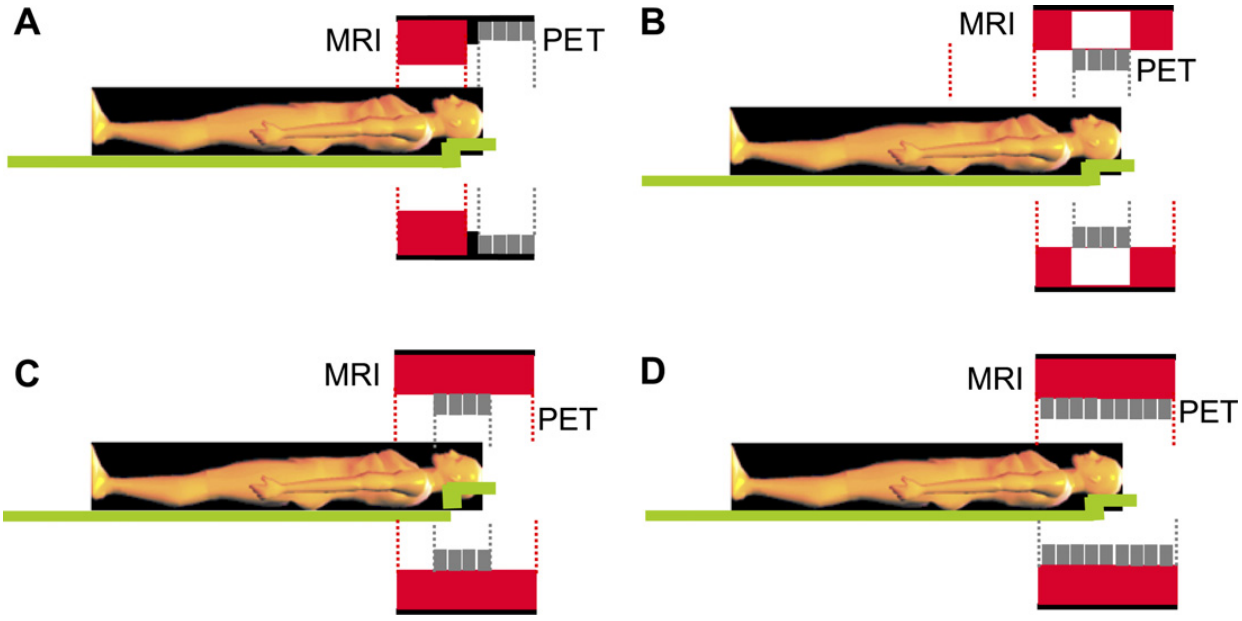

Fig. 6. Concept of PET/MRI illustrated through four potential designs that are being explored. (*A*) Two scanners mounted together back-to-back allow sequential rather than simultaneous acquisition like PET/CT. (*B*) PET scanner inserted within a gap in a superconducting magnet where the PMTs can be placed in a low magnetic field through a combination of magnet design and the use of fiberoptic bundles. (*C*) PET scanner inserted (between the RF-coil and gradient set of the MR system) into a standard clinical MRI system. (*D*) Full integration of a whole-body PET/MRI system.

the design of combined PET/MR scanners [138] because they significantly reduce the amount of electronics needed inside the MRI [139]. SiPMs are currently commercially available from several vendors such as Photonique (Geneva, Switzerland), a distributor for CPTA Russia (http://www.photonique.ch), Hamamatsu, (Hamamatsu City, Japan), (http://www.hamamatsu.com), or SensL, (Blackrock, Cork, Ireland) (http://www.sensl.com). The development of combined PET/MR systems based on APDs is one of the most promising designs achieved thus far. The first in vivo mice images confirmed the capability of the system for performing simultaneous PET/MR imaging [137]. Further experimental analysis showed that both systems work with unhindered performance, consolidating the observation that each modality is virtually invisible to the other.

The conceptual design of combined PET/MR instrumentation for humans would greatly benefit from the experience gained in preclinical imaging. There are at least four evident ways to combine PET and MRI in a single gantry (Fig. 6). The obvious and easiest configuration would be to combine PET/MRI as two "standard" scanners hardware wired to each other with a common bed and common computer console similar to PET/CT (Fig. 6A). This configuration would be more straightforward to develop when compared with fully integrated approaches, because the PET electronics are outside the MRI scanner's field of view and high magnetic field. The main limitation of this design is that the PET and MR data will be acquired sequentially rather than simultaneously, seriously limiting the envisioned applications (eg, the assessment of two independent functional processes with PET tracers and MRI contrast agents [functional MRI or MR spectroscopy]). Moreover, MRI has relatively long acquisition times when compared with CT, which further emphasizes the advantages of simultaneous scanning to reduce acquisition time.

The full integration of PET and MRI with large and matched fields of view in a single gantry to allow simultaneous whole-body scanning remains the long-term objective (Fig. 6D); however, the cost and complexity of designing and manufacturing such a large-scale system makes an initial smaller-scale design appealing. As a result of a close collaboration between Siemens Medical Solutions (Erlangen, Germany) and the University of Tuebingen, Germany, the first prototype human PET insert, the BrainPET scanner [140,141], was designed in 2005 using photodetectors insensitive to magnetic fields (APDs instead of PMTs) and non-magnetic detector and front-end electronic materials to operate within a clinical MRI system, namely, the 3T TIM Trio manufactured by the same company. The BrainPET was designed to work quietly in the frequency range of interest for MRI at 3 T, rendering it well-matched with the most sophisticated MR brain sequences that can be performed at this field strength. The first patient images were shown late in 2006. The system is currently undergoing a detailed evaluation of mutual interference between

the two imaging modalities and is being used comprehensively to assess its potential using normal subjects and clinical studies [142].

The role of advanced molecular imaging instrumentation in biomedical research

The introduction of FDG and a multitude of novel radiotracers has demonstrated the enormous potential of nuclear medicine as an emerging discipline in the field of molecular imaging [143]. Molecular imaging in its broad definition represents methodologies and probes that allow visualizing events at the cellular and molecular levels [144]. The intended targets for this purpose include cell surface receptors, transporters, intracellular enzymes, or messenger RNA. The source of the signal detected by these techniques could originate directly from the molecule or its surrogates.

Molecular imaging is the main focus of the NIH Road Map Initiative, a major undertaking, further demonstrating the importance of this approach in the scientific community [145]. It is not farfetched to speculate that, in the future, molecular imaging will be the centerpiece of medical practice whereby early and accurate diagnoses will be made by appropriate imaging probes. Treatment for most diseases and disorders would be individualized by using labeled pharmacologic agents as tracers that would be predictive of a favorable outcome from therapeutic doses of compounds [146]. Molecular and cellular imaging techniques would be successfully employed for monitoring response and detecting early evidence of failure or recurrence of disease activity. In addition to nuclear medicine techniques, many different methodologies have been studied for the purpose of molecular imaging, including optical imaging, MR spectroscopy, and functional MRI. The merits and current applications of these techniques are described elsewhere in the literature [147,148].

The challenges faced by the imaging community include a shortage of properly trained personnel to perform various tasks that are associated with the very complex technology. These tasks include running cyclotron facilities, synthesizing routine and new novel compounds, and operating the imaging instruments. Obviously, there is a great demand for physicians and scientists who are adequately trained to provide this type of service with high standards. Understanding and providing quantitative data for accurate diagnosis and treatment is a major challenge that scientists and physicians face in this discipline.

It can arguably be stated that FDG-PET, as a single modality, has made a lasting impact on the specialty of nuclear medicine. In fact, it has rejuvenated the field and has changed its image in the medical community. It is not an exaggeration to speculate that, in the coming years, the number of FDG-PET images performed in most facilities will exceed that of all other procedures performed with radiolabeled compounds. It is appropriate to applaud our distinguished colleague Henry Wagner, who named FDG as the "Molecule of the Century" because of its unparalleled impact on the evolution of the specialty of nuclear medicine.

Summary

An overview of current state-of-the art developments in stand-alone PET and emerging dual-modality (PET/CT and PET/MR) instrumentation is provided in this review. Many different design paths have been tried and continue to be pursued in academic and corporate settings that offer different compromises in terms of performance and versatility but in most cases improve the clinical workflow efficiency. It is still uncertain which designs will be incorporated into future clinical systems, but it is certain that technological advances will continue and will enable new quantitative capabilities in molecular imaging using PET. More compact and cost-effective designs of dual-modality systems are being explored using a rail-with-sliding-bed approach in which a sliding CT bed is placed on a track in the floor and linked to a flexible SPECT camera [149]. Various other rail-based, docking, and click-over approaches for anatomolecular imaging fusion are also being considered for which the possibilities are limited only by the imagination and creativity of researchers [150]. In any approach, it is the power of molecular imaging using highly specific tracers that is central and not the number of slices of the CT subsystem when considering the example of combined PET/CT.

References

[1] Jones T. Molecular imaging with PET—the future challenges. Br J Radiol 2002;75:6S–15S.
[2] Phelps ME. PET: the merging of biology and imaging into molecular imaging. J Nucl Med 2000; 41:661–81.
[3] Nutt R. The history of positron emission tomography. Mol Imaging Biol 2002;4:11–26.
[4] Alavi A, Reivich M. Guest editorial: the conception of FDG-PET imaging. Semin Nucl Med 2002;32:2–5.
[5] Czernin J, Allen-Auerbach M, Schelbert HR. Improvements in cancer staging with PET/CT: literature-based evidence as of September 2006. J Nucl Med 2007;48:78S–88S.
[6] Beyer T, Townsend DW, Brun T, et al. A combined PET/CT scanner for clinical oncology. J Nucl Med 2000;41:1369–79.

[7] Marsden PK, Strul D, Keevil SF, et al. Simultaneous PET and NMR. Br J Radiol 2002;75: S53–9.
[8] Cherry SR. Multimodality in vivo imaging systems: twice the power or double the trouble? Annu Rev Biomed Eng 2006;8:35–62.
[9] Wrenn FR Jr, Good ML, Handler P. The use of positron-emitting radioisotopes for the localization of brain tumors. Science 1951;113:525–7.
[10] Sweet WH. The uses of nuclear disintegration in the diagnosis and treatment of brain tumor. N Engl J Med 1951;245:875–8.
[11] Brownell GL, Sweet WH. Localization of brain tumors with positron emitters. Nucleonics 1953;11:40–5.
[12] Phelps ME, Hoffman EJ, Mullani NA, et al. Design considerations for a positron emission transaxial tomograph (PETT III). IEEE Tran Nucl Sci 1976;23:516–22.
[13] Hoffman EJ, Phelps ME, Mullani NA, et al. Design and performance characteristics of a whole-body transaxial tomograph. J Nucl Med 1976;17:493–502.
[14] Jones T, Chesler DA, Ter-Pogossian MM. The continuous inhalation of oxygen-15 for assessing regional oxygen extraction in the brain of man. Br J Radiol 1976;49:339–43.
[15] Thompson CJ, Yamamoto YL, Meyer E. Positome II: a high efficiency positron imaging device for dynamic brain studies. IEEE Trans Nucl Sci 1979;26:583–9.
[16] Ter-Pogossian MM, Mullani NA, Hood JT, et al. Design considerations for a positron emission transverse tomograph (PETT V) for imaging of the brain. J Comput Assist Tomogr 1978;2: 539–44.
[17] Ter-Pogossian MM, Ficke DC, Hood JT Sr, et al. PETT VI: a positron emission tomograph utilizing cesium fluoride scintillation detectors. J Comput Assist Tomogr 1982;6:125–33.
[18] Wienhard K, Schmand M, Casey ME, et al. The ECAT HRRT: performance and first clinical application of the new high resolution research tomograph. IEEE Trans Nucl Sci 2002;49:104–10.
[19] Thompson CJ. Instrumentation for positron emission mammography. PET Clinics 2006;1: 33–8.
[20] Daube-Witherspoon ME, Carson RE, Yan YC, et al. Scatter correction in maximum-likelihood reconstruction of PET data. Conference Record of IEEE Nuclear Science Symposium and Medical Imaging Conference 1992;2:945–7.
[21] Surti S, Karp J, Muehllehner G, et al. Investigation of Lanthanum scintillators for 3-D PET. IEEE Trans Nucl Sci 2003;50:348–54.
[22] Melcher CL. Perspectives on the future development of new scintillators. Nucl Instrum Methods Phys Res A 2005;537:6–14.
[23] Surti S, Kuhn A, Werner ME, et al. Performance of Philips Gemini TF PET/CT scanner with special consideration for its time-of-flight imaging capabilities. J Nucl Med 2007;48:471–80.
[24] Marsden PK. Detector technology challenges for nuclear medicine and PET. Nucl Instr Methods A 2003;513:1–7.
[25] Derenzo SE, Weber MJ, Bourret-Courchesne E, et al. The quest for the ideal inorganic scintillator. Nucl Instr Meth A 2003;505:111–7.
[26] van Eijk CWE. Inorganic scintillators in medical imaging. Phys Med Biol 2002;47:R85–R106.
[27] Dahlbom M, MacDonald LR, Schmand M, et al. A YSO/LSO phoswich array detector for single and coincidence photon imaging. IEEE Trans Nucl Sci 1998;45:1128–32.
[28] Braem A, Chamizo Llatas M, Chesi E, et al. Feasibility of a novel design of high-resolution parallax-free Compton enhanced PET scanner dedicated to brain research. Phys Med Biol 2004;49:2547–62.
[29] Seguinot J, Braem A, Chesi E, et al. Novel geometrical concept of high performance brain PET scanner: principle, design and performance estimates. Nuovo Cimento C 2006;29: 429–63.
[30] Lewellen TK. Time-of-flight PET. Semin Nucl Med 1998;28:268–75.
[31] Moses WW. Time of flight in PET revisited. IEEE Trans Nucl Sci 2003;50:1325–30.
[32] Ter-Pogossian MM, Mullani NA, Ficke DC, et al. Photon time-of-flight-assisted positron emission tomography. J Comput Assist Tomogr 1981;5:227–39.
[33] Conti M, Bendriem B, Casey M, et al. First experimental results of time-of-flight reconstruction on an LSO PET scanner. Phys Med Biol 2005;50:4507–26.
[34] Harrison RL, Gillispie SB, Alessio AM, et al. The effects of object size, attenuation, scatter, and random coincidences on signal to noise ratio in simulations of time-of-flight positron emission tomography. IEEE Nuclear Science Symposium Conference Record. October 23–29, 2005, Puerto Rico.
[35] Surti S, Karp JS, Popescu LM, et al. Investigation of time-of-flight benefit for fully 3-D PET. IEEE Trans Med Imaging 2006;25:529–38.
[36] Watson CC, Casey ME, Erikksson L, et al. NEMA NU 2 performance tests for scanners with intrinsic radioactivity. J Nucl Med 2004; 45:822–6.
[37] Bettinardi V, Danna M, Savi A, et al. Performance evaluation of the new whole-body PET/CT scanner: discovery ST. Eur J Nucl Med Mol Imaging 2004;31:867–81.
[38] Mawlawi O, Podoloff DA, Kohlmyer S, et al. Performance characteristics of a newly developed PET/CT scanner using NEMA standards in 2D and 3D modes. J Nucl Med 2004;45: 1734–42.
[39] Erdi YE, Nehmeh SA, Mulnix T, et al. PET performance measurements for an LSO-based combined PET/CT scanner using the National Electrical Manufacturers Association NU 2-2001 standard. J Nucl Med 2004;45:813–21.

[40] Surti S, Karp JS. Imaging characteristics of a 3-dimensional GSO whole-body PET camera. J Nucl Med 2004;45:1040–9.
[41] Brambilla M, Secco C, Dominietto M, et al. Performance characteristics obtained for a new 3-dimensional lutetium oxyorthosilicate-based whole-body PET/CT scanner with the National Electrical Manufacturers Association NU 2-2001 standard. J Nucl Med 2005; 46:2083–91.
[42] Kemp BJ, Kim C, Williams JJ, et al. NEMA NU 2-2001 performance measurements of an LYSO-based PET/CT system in 2D and 3D acquisition modes. J Nucl Med 2006;47:1960–7.
[43] Matsumoto K, Kitamura K, Mizuta T, et al. Performance characteristics of a new 3-dimensional continuous-emission and spiral-transmission high-sensitivity and high-resolution PET camera evaluated with the NEMA NU 2-2001 standard. J Nucl Med 2006;47:83–90.
[44] Bentourkia M, Laribi M, Lakinsky E, et al. Scatter restoration in PET imaging. IEEE Nuclear Science Symposium Conference Record 1992; 2:1075–9.
[45] Watanabe M, Shimizu K, Omura T, et al. A new high-resolution PET scanner dedicated to brain research. IEEE Trans Nucl Sci 2002; 49:634–9.
[46] Karp JS, Surti S, Daube-Witherspoon ME, et al. Performance of a brain PET camera based on anger-logic gadolinium oxyorthosilicate detectors. J Nucl Med 2003;44:1340–9.
[47] Braem A, Chamizo Llatas M, Chesi E, et al. Novel design of a parallax free Compton enhanced PET scanner. Nucl Instr Methods A 2004;525:268–74.
[48] Zaidi H, Montandon M-L. The new challenges of brain PET imaging technology. Curr Med Imag Rev 2006;2:3–13.
[49] Doshi NK, Silverman RW, Shao Y, et al. max-PET, a dedicated mammary and axillary region PET imaging system for breast cancer. IEEE Trans Nucl Sci 2001;48:811–5.
[50] Freifelder R, Karp JS. Dedicated PET scanners for breast imaging. Phys Med Biol 1997;42: 2463–80.
[51] Levine EA, Freimanis RI, Perrier ND, et al. Positron emission mammography: initial clinical results. Ann Surg Oncol 2003;10:86–91.
[52] Moses WW, Qi J. Instrumentation optimization for positron emission mammography. Nucl Instr Meth A 2004;527:76–82.
[53] Murthy K, Aznar M, Bergman AM, et al. Positron emission mammographic instrument: initial results. Radiology 2000;215:280–5.
[54] Raylman RR, Majewski S, Wojcik R, et al. The potential role of positron emission mammography for detection of breast cancer: a phantom study. Med Phys 2000;27:1943–54.
[55] Smith MF, Raylman RR, Majewski S, et al. Positron emission mammography with tomographic acquisition using dual planar detectors: initial evaluations. Phys Med Biol 2004;49:2437–52.
[56] Chen H-T, Kao C-M, Chen C-T. A fast, energy-dependent scatter reduction method for 3D PET imaging. IEEE Nuclear Science Symposium Conference Record 2003;4:2630–4.
[57] Weinberg IN, Beylin D, Zavarzin V, et al. Positron emission mammography: high-resolution biochemical breast imaging. Technol Cancer Res Treat 2005;4:55–60.
[58] Zhang J, Olcott PD, Chinn G, et al. Study of the performance of a novel 1 mm resolution dual-panel PET camera design dedicated to breast cancer imaging using Monte Carlo simulation. Med Phys 2007;34:689–702.
[59] Belcari N, Camarda M, Del Guerra A, et al. Detector development for a novel positron emission mammography scanner based on YAP:Ce crystals. Nucl Instr Meth A 2004;525:258–62.
[60] Holdsworth CH, Badawi RD, Santos P, et al. Evaluation of a Monte Carlo scatter correction in clinical 3D PET. Conference Record IEEE Nuclear Science Symposium 2003;4:2540–4.
[61] Karp JS, Freifelder R, Geagan MJ, et al. Three-dimensional imaging characteristics of the HEAD PENN-PET scanner. J Nucl Med 1997;38: 636–43.
[62] Adam LE, Karp JS, Daube-Witherspoon ME, et al. Performance of a whole-body PET scanner using curve-plate NaI(Tl) detectors. J Nucl Med 2001;42:1821–30.
[63] Phelps ME, Cherry SR. The changing design of positron imaging systems. Clin Positron Imaging 1998;1:31–45.
[64] Hasegawa B, Zaidi H. Dual-modality imaging: more than the sum of its components. In: Zaidi H, editor. Quantitative analysis in nuclear medicine imaging. New York: Springer; 2006. p. 35–81.
[65] Hasegawa BH, Gingold EL, Reilly SM, et al. Description of a simultaneous emission-transmission CT system. Proc SPIE 1990;1231:50–60.
[66] Tsoumpas C, Aguiar P, Ros D, et al. Scatter simulation including double scatter. Conference Record of the IEEE Nuclear Science Symposium 2005;3:5.
[67] Watson CC, Casey ME, Michel C, et al. Advances in scatter correction for 3D PET/CT. Conference Record of the IEEE Nuclear Science Symposium 2004;5:3008–12.
[68] Maes F, Vandermeulen D, Suetens P. Medical image registration using mutual information. Proc IEEE 2003;91:1699–722.
[69] Watson CC. Extension of single scatter simulation to scatter correction of time-of-flight PET. Conference Record of the IEEE Nuclear Science Symposium 2005;5:2492–6.
[70] Werner ME, Surti S, Karp JS. Implementation and evaluation of a 3D PET single scatter simulation with TOF modeling. Conference Record of the IEEE Nuclear Science Symposium 2006; 3:1768–73.

[71] Pietrzyk U, Herholz K, Fink G, et al. An interactive technique for three-dimensional image registration: validation for PET, SPECT, MRI and CT brain studies. J Nucl Med 1994;35:2011–8.
[72] Woods RP, Grafton ST, Holmes CJ, et al. Automated image registration. I. General methods and intrasubject, intramodality validation. J Comput Assist Tomogr 1998;22:139–52.
[73] Krishnasetty V, Fischman AJ, Halpern EL, et al. Comparison of alignment of computer-registered data sets: combined PET/CT versus independent PET and CT of the thorax. Radiology 2005;237:635–9.
[74] Slomka PJ. Software approach to merging molecular with anatomic information. J Nucl Med 2004;45(Suppl 1):36S–45S.
[75] Townsend DW, Carney JPJ, Yap JT, et al. PET/CT today and tomorrow. J Nucl Med 2004;45: 4S–14S.
[76] Lardinois D, Weder W, Hany TF, et al. Staging of non–small-cell lung cancer with integrated positron-emission tomography and computed tomography. N Engl J Med 2003;348:2500–7.
[77] Kinahan PE, Hasegawa BH, Beyer T. X-ray–based attenuation correction for positron emission tomography/computed tomography scanners. Semin Nucl Med 2003;33:166–79.
[78] Zaidi H, Koral KF. Scatter modelling and compensation in emission tomography. Eur J Nucl Med Mol Imaging 2004;31:761–82.
[79] Comtat C, Kinahan PE, Fessler JA, et al. Clinically feasible reconstruction of 3D whole-body PET/CT data using blurred anatomical labels. Phys Med Biol 2002;47:1–20.
[80] Goerres GW, Burger C, Kamel E, et al. Respiration-induced attenuation artifact at PET/CT: technical considerations. Radiology 2003;226: 906–10.
[81] Osman MM, Cohade C, Nakamoto Y, et al. Respiratory motion artifacts on PET emission images obtained using CT attenuation correction on PET-CT. Eur J Nucl Med Mol Imaging 2003;30:603–6.
[82] Papathanassiou D, Becker S, Amir R, et al. Respiratory motion artifact in the liver dome on FDG PET/CT: comparison of attenuation correction with CT and a caesium external source. Eur J Nucl Med Mol Imaging 2005;32:1422–8.
[83] Gould KL, Pan T, Loghin C, et al. Frequent diagnostic errors in cardiac PET/CT due to misregistration of CT attenuation and emission PET images: a definitive analysis of causes, consequences, and corrections. J Nucl Med 2007;48: 1112–21.
[84] Goetze S, Brown TL, Lavely WC, et al. Attenuation correction in myocardial perfusion SPECT/CT: effects of misregistration and value of reregistration. J Nucl Med 2007;48:1090–5.
[85] Pan T, Mawlawi O, Nehmeh SA, et al. Attenuation correction of PET images with respiration-averaged CT images in PET/CT. J Nucl Med 2005;46:1481–7.
[86] Sourbelle K, Kachelriess M, Kalender WA. Reconstruction from truncated projections in CT using adaptive detruncation. Eur Radiol 2005; 15:1008–14.
[87] Michel C, Noo F, Sibomana M, et al. An iterative method for creating attenuation maps from highly truncated CT data. Noo F, Kudo H, Zeng L, editors. Proceedings of the 8th international meeting on fully 3-D image reconstruction in radiology and nuclear medicine. Utah; 2005. p. 88–91.
[88] Mawlawi O, Erasmus JJ, Pan T, et al. Truncation artifact on PET/CT: impact on measurements of activity concentration and assessment of a correction algorithm. AJR Am J Roentgenol 2006; 186:1458–67.
[89] Beyer T, Bockisch A, Kuhl H, et al. Whole-body 18F-FDG PET/CT in the presence of truncation artifacts. J Nucl Med 2006;47:91–9.
[90] Dizendorf E, Hany TF, Buck A, et al. Cause and magnitude of the error induced by oral CT contrast agent in CT-based attenuation correction of PET emission studies. J Nucl Med 2003;44: 732–8.
[91] Antoch G, Freudenberg LS, Egelhof T, et al. Focal tracer uptake: a potential artifact in contrast-enhanced dual-modality PET/CT scans. J Nucl Med 2002;43:1339–42.
[92] Antoch G, Freudenberg LS, Beyer T, et al. To enhance or not to enhance? 18F-FDG and CT contrast agents in dual-modality 18F-FDG PET/CT. J Nucl Med 2004;45(Suppl 1):56S–65S.
[93] Antoch G, Kuehl H, Kanja J, et al. Dual-modality PET/CT scanning with negative oral contrast agent to avoid artifacts: introduction and evaluation. Radiology 2004;230:879–85.
[94] Nehmeh SA, Erdi YE, Kalaigian H, et al. Correction for oral contrast artifacts in CT attenuation-corrected PET images obtained by combined PET/CT. J Nucl Med 2003;44:1940–4.
[95] Nakamoto Y, Chin BB, Kraitchman DL, et al. Effects of nonionic intravenous contrast agents in PET/CT imaging: phantom and canine studies. Radiology 2003;227:817–24.
[96] Yau Y-Y, Chan W-S, Tam Y-M, et al. Application of intravenous contrast in PET/CT: does it really introduce significant attenuation correction error? J Nucl Med 2005;46:283–91.
[97] Berthelsen AK, Holm S, Loft A, et al. PET/CT with intravenous contrast can be used for PET attenuation correction in cancer patients. Eur J Nucl Med Mol Imaging 2005;32:1167–75.
[98] Groves AM, Kayani I, Dickson JC, et al. Oral contrast medium in PET/CT: should you or shouldn't you? Eur J Nucl Med Mol Imaging 2005;32:1160–6.
[99] Beyer T, Antoch G, Bockisch A, et al. Optimized intravenous contrast administration for diagnostic whole-body 18F-FDG PET/CT. J Nucl Med 2005;46:429–35.
[100] Heiba SI, Luo J, Sadek S, et al. Attenuation-correction induced artifact in F-18 FDG PET

imaging following total knee replacement. Clin Positron Imaging 2000;3:237–9.
[101] Halpern BS, Dahlbom M, Waldherr C, et al. Cardiac pacemakers and central venous lines can induce focal artifacts on CT-corrected PET images. J Nucl Med 2004;45:290–3.
[102] DiFilippo FP, Brunken RC. Do implanted pacemaker leads and ICD leads cause metal-related artifact in cardiac PET/CT? J Nucl Med 2005; 46:436–43.
[103] Goerres GW, Hany TF, Kamel E, et al. Head and neck imaging with PET and PET/CT: artifacts from dental metallic implants. Eur J Nucl Med Mol Imaging 2002;29:367–70.
[104] Goerres GW, Ziegler SI, Burger C, et al. Artifacts at PET and PET/CT caused by metallic hip prosthetic material. Radiology 2003;226:577–84.
[105] Kamel EM, Burger C, Buck A, et al. Impact of metallic dental implants on CT-based attenuation correction in a combined PET/CT scanner. Eur Radiol 2003;13:724–8.
[106] Bujenovic S, Mannting F, Chakrabarti R, et al. Artifactual 2-deoxy-2-[(18)F]fluoro-D-glucose localization surrounding metallic objects in a PET/CT scanner using CT-based attenuation correction. Mol Imaging Biol 2003;5:20–2.
[107] Lemmens C, Montandon M-L, Nuyts J, et al. Impact of metal artifacts due to EEG electrodes in brain PET imaging. Proceedings of IEEE Nuclear Science Symposium and Medical Imaging Conference 2007; in press.
[108] Hsieh J, Molthen RC, Dawson CA, et al. An iterative approach to the beam hardening correction in cone beam CT. Med Phys 2000;27: 23–9.
[109] Kachelrieb M, Kalender WA. Improving PET/CT attenuation correction with iterative CT beam hardening correction. IEEE Nuclear Science Symposium Conference Record. October 23–29, 2005, Puerto Rico.
[110] Ay M, Zaidi H. Assessment of errors caused by x-ray scatter and use of contrast medium when using CT-based attenuation correction in PET. Eur J Nucl Med Mol Imaging 2006;33:1301–13.
[111] Siewerdsen JH, Daly MJ, Bakhtiar B, et al. A simple, direct method for x-ray scatter estimation and correction in digital radiography and cone-beam CT. Med Phys 2006;33:187–97.
[112] Malusek A, Seger MM, Sandborg M, et al. Effect of scatter on reconstructed image quality in cone beam computed tomography: evaluation of a scatter-reduction optimisation function. Radiat Prot Dosimetry 2005;114:337–40.
[113] Wiley G. Disruptive technology: the conflict over PET/CT. Imaging Economics 2005;18: 17–20.
[114] Zaidi H. The quest for the ideal anato-molecular imaging fusion tool. Biomed Imaging Interv J 2006;2:e47.
[115] Alavi A, Mavi A, Basu S, et al. Is PET-CT the only option?. [editorial]. Eur J Nucl Med Mol Imaging 2007;34:819–21.
[116] Beyer T, Townsend D. Putting 'clear' into nuclear medicine: a decade of PET/CT development. Eur J Nucl Med Mol Imaging 2006;33: 857–61.
[117] Vogel WV, Oyen WJ, Barentsz JO, et al. PET/CT: panacea, redundancy, or something in between? J Nucl Med 2004;45(Suppl 1):15S–24S.
[118] Blodgett TM, Casagranda B, Townsend DW, et al. Issues, controversies, and clinical utility of combined PET/CT imaging: what is the interpreting physician facing? AJR Am J Roentgenol 2005;184:S138–45.
[119] Xing L, Wessels B. The value of PET/CT is being over-sold as a clinical tool in radiation oncology. Med Phys 2005;32:1457–9.
[120] Jager PL, Slart RH, Corstens F, et al. PET-CT: a matter of opinion? Eur J Nucl Med Mol Imaging 2003;30:470–1 [author reply: 471].
[121] Lemke AJ, Niehues SM, Hosten N, et al. Retrospective digital image fusion of multidetector CT and 18F-FDG PET: clinical value in pancreatic lesions—a prospective study with 104 patients. J Nucl Med 2004;45:1279–86.
[122] Zaidi H, Mawlawi O, Orton CG. Point/counterpoint. Simultaneous PET/MR will replace PET/CT as the molecular multimodality imaging platform of choice. Med Phys 2007;34: 1525–8.
[123] Hammer BE, Christensen NL, Heil BG. Use of a magnetic field to increase the spatial resolution of positron emission tomography. Med Phys 1994;21:1917–20.
[124] Christensen NL, Hammer BE, Heil BG, et al. Positron emission tomography within a magnetic field using photomultiplier tubes and light-guides. Phys Med Biol 1995;40:691–7.
[125] Raylman RR, Hammer BE, Christensen NL. Combined MRI-PET scanner: a Monte-Carlo evaluation of the improvements in PET resolution due to the effects of a static homogeneous magnetic field. IEEE Trans Nucl Sci 1996;43: 2406–12.
[126] Shao Y, Cherry SR, Farahani K, et al. Simultaneous PET and MR imaging. Phys Med Biol 1997;42:1965–70.
[127] Slates R, Farahani K, Shao Y, et al. A study of artifacts in simultaneous PET and MR imaging using a prototype MR compatible PET scanner. Phys Med Biol 1999;44:2015–27.
[128] Mackewn JE, Strul D, Hallett WA, et al. Design and development of an MR-compatible PET scanner for imaging small animals. IEEE Trans Nucl Sci 2005;52:1376–80.
[129] Yamamoto S, Takamatsu S, Murayama H, et al. A block detector for a multislice, depth-of-interaction MR-compatible PET. EEE Trans Nucl Sci 2005;52:33–7.
[130] Raylman RR, Majewski S, Lemieux SK, et al. Simultaneous MRI and PET imaging of a rat brain. Phys Med Biol 2006;51:6371–9.
[131] Raylman RR, Majewski S, Velan SS, et al. Simultaneous acquisition of magnetic resonance

spectroscopy (MRS) data and positron emission tomography (PET) images with a prototype MR-compatible, small animal PET imager. J Magn Reson 2007;186:305–10.
[132] Lucas AJ, Hawkes RC, Ansorge RE, et al. Development of a combined microPET-MR system. Technol Cancer Res Treat 2006;5:337–41.
[133] Handler WB, Gilbert KM, Peng H, et al. Simulation of scattering and attenuation of 511 keV photons in a combined PET/field-cycled MRI system. Phys Med Biol 2006;51:2479–91.
[134] Dumouchel T, Bergeron M, Cadorette J, et al. Initial performance assessment of the LabPET APD-based digital PET scanner. [abstract]. J Nucl Med 2007;48:39P.
[135] Catana C, Wu Y, Judenhofer MS, et al. Simultaneous acquisition of multislice PET and MR images: initial results with a MR-compatible PET scanner. J Nucl Med 2006;47:1968–76.
[136] Pichler BJ, Judenhofer MS, Catana C, et al. Performance test of an LSO-APD detector in a 7-T MRI scanner for simultaneous PET/MRI. J Nucl Med 2006;47:639–47.
[137] Judenhofer MS, Catana C, Swann BK, et al. Simultaneous PET/MR images, acquired with a compact MRI compatible PET detector in a 7 Tesla magnet. Radiology 2007;244:807–14.
[138] Dolgoshein B, et al. Status report on Silicon photomultiplier development and its applications. Nuclear Instr Meth A 2006;563: 368–76.
[139] Moehrs S, Del Guerra A, Herbert DJ, et al. A detector head design for small-animal PET with silicon photomultipliers (SiPM). Phys Med Biol 2006;51:1113–27.
[140] Grazioso R, Zhang N, Corbeil J, et al. APD-based PET detector for simultaneous PET/MR imaging. Presented at the IEEE Nuclear Science Symposium and Medical Imaging Conference, October 23–29, 2005, Puerto Rico, USA.
[141] Burbar Z, Grazioso RF, Corbeil J, et al. PET performance of MR/PET brain insert tomograph. Presented at the IEEE Nuclear Science Symposium and Medical Imaging Conference, October 29–November 4, 2006, San Diego, CA.
[142] Schlemmer H, Pichler BJ, Wienhard K, et al. Simultaneous MR/PET for brain imaging: first patient scans. [abstract]. J Nucl Med 2007; 48:45P.
[143] Torigian DA, Huang SS, Houseni M, et al. Functional imaging of cancer with emphasis on molecular techniques. CA Cancer J Clin 2007;57: 206–24.
[144] Weissleder R, Mahmood U. Molecular imaging. Radiology 2001;219:316–33.
[145] Zerhouni E. Medicine. The NIH Roadmap. Science 2003;302:63–72.
[146] Pickles MD, Gibbs P, Lowry M, et al. Diffusion changes precede size reduction in neoadjuvant treatment of breast cancer. Magn Reson Imaging 2006;24:843–7.
[147] Intes X, Chance B. Non-PET functional imaging techniques: optical. Radiol Clin North Am 2005;43:221–34.
[148] Delikatny EJ, Poptani H. MR techniques for in vivo molecular and cellular imaging. Radiol Clin North Am 2005;43:205–20.
[149] Bailey D, Roach P, Bailey E, et al. Development of a cost-effective modular SPECT/CT scanner. Eur J Nucl Med Mol Imaging 2007; 34:1415–26.
[150] Beekman F, Hutton B. Multi-modality imaging on track. Eur J Nucl Med Mol Imaging 2007; 34:1410–4.